View metadata, citation and similar papers at core.ac.uk
brought to you by CORE
provided by Columbia University Academic Commons

The Meteoritical Society

*Meteoritics & Planetary Science* 1–8 (2014)
doi: 10.1111/maps.12372

# H, not O or pressure, causes eutectic *T* depression in the Fe-FeS System to 8 GPa

Antonio S. BUONO and David WALKER*

Lamont Doherty Earth Observatory, Department of Earth and Environmental Sciences, Columbia University, Palisades, New York 10964, USA
*Corresponding author. E-mail: dwalker@ldeo.columbia.edu

(*Received 23 January 2014; revision accepted 01 August 2014*)

**Abstract**–The Fe-FeS system maintains a eutectic temperature of 990 ± 10 °C to at least 8 GPa if starting materials and pressure media are rigorously dehydrated. Literature reports of pressure-induced freezing point depression of the eutectic for the Fe-FeS system are not confirmed. Modest addition of oxygen alone is confirmed to cause negligible freezing point depression at 6 GPa. Addition of H alone causes a progressive decrease in the eutectic temperature with *P* in the Fe-FeS-H system to below 965 °C at 6 GPa to below 950 °C at 8 GPa. It is our hypothesis that moisture contamination in unrigorously dried experiments may be an H source for freezing point depression. O released from $H_2O$ disproportionation reacts with Fe and is sequestered as ferropericlase along the sample capsules walls, leaving the H to escape the system and/or enter the Fe-FeS mixture. The observed occurrence of ferropericlase on undried MgO capsule margins is otherwise difficult to explain, because an alternate source for the oxygen in the ferropericlase layer is difficult to identify. This study questions the use of pressure-depressed Fe-S eutectic temperatures and suggests that the lower eutectic temperatures sometimes reported are achieved by moving into the ternary Fe-S-H system. These results adjust slightly the constraints on eutectic temperatures allowed for partly solidified cores on small planets. H substantially diminishes the temperature extent of the melting interval in Fe-S by reducing the melting points of the crystalline phases more than it depresses the eutectic.

## INTRODUCTION

Earth's outer core is 5–10% less dense than pure metallic Fe-Ni liquid (Birch 1964; Anderson and Isaak 2002). The outer core composition may have approximately 10% light elements (Birch 1952, 1964). The proposed light elements are probably some combination of sulfur (S), carbon (C), oxygen (O), hydrogen (H), and silicon (Si) (Stevenson 1987; Poirier 1994; Hillgren et al. 2000; Li and Fei 2003). The composition of the core has some influence on the global geochemical balance (McDonough 2003). These considerations are also relevant to which alloying elements may be present in the cores of other planetary bodies, including the terrestrial planets such as Mercury, Mars (Morgan and Anders 1980; Sanloup et al. 1999; Stevenson 2001, 2010), and bodies beyond the asteroid belt, including Jupiter's moons Io, Ganymede, and Europa (Anderson et al. 1996, 1997, 2001).

S is the light element candidate most often considered as a binary alloying agent for inclusion in the metallic cores of rocky planets. When considering a simple system like Fe-S, the most important point in the phase diagram is the point of first melt. This point, the eutectic, indicates the lowest temperature at which a planetary interior can be and still contain a solid metallic inner core with a liquid outer core.

Many studies have looked at the Fe-S binary system at a range of *P*–*T* conditions (Ryzhenko and Kennedy 1973; Usselman 1975; Urakawa et al. 1987; Fei et al. 1997; Morard et al. 2007; Buono and Walker 2011). These studies show several different results for the effect of pressure on the eutectic temperature (*T*) and composition (x). In this paper, we conduct new high-pressure experiments in the Fe-S, Fe-S-H, and Fe-S-O systems to shed some light on the effects of pressure, O, and H on the eutectic and compare our results with literature data to understand the source of



© The Meteoritical Society, 2014.

Table 1. Run conditions and starting compositions.

| Sample | Starting composition | $P$ (GPa) | Heater type | $T$ (°C) | Run duration min | Phases |
|---|---|---|---|---|---|---|
| GG-1015 | Brucite + $MgH_2$ in Pt | 6 | $LaCrO_3$ | 800 | 5 | Periclase |
| GG-1016 | Brucite + $MgH_2$ in Au | 6 | $LaCrO_3$ | 600 | 15 | Periclase |
| BB-881 | 87 wt% Fe + 13 wt% S | 6 | $LaCrO_3$ | 980 | 177 | Un-melted |
| BB-888 | 87 wt% Fe + 13 wt% S | 6 | $LaCrO_3$ | 1000 | 138 | S-L + Fe |
| BB-1004 | 87 wt% Fe + 13 wt% S | **8** | Re | 980 | 326 | Un-melted |
| BB-1006 | 87 wt% Fe + 13 wt% S | **8** | Re | 995 | 1154 | S-L + Fe + Un-melted |
| BB-1008 | 87 wt% Fe + 13 wt% S | 8 | Re | 1015 | 1309 | S-L + Fe + Un-melted |
| BB-875 | 85 wt% Fe + 11 wt% S + 4 wt% O | 6 | $LaCrO_3$ | 980 | 95 | Un-melted |
| TT-799 | 85 wt% Fe + 11 wt% S + 4 wt% O | 6 | $LaCrO_3$ | 1000 | 1490 | S-L + O-L + Fe + Un-melted |
| GG-1012 | 85 wt% Fe + 11 wt% S + 4 wt% O | 6 | $LaCrO_3$ | 1100 | 1159 | S-L + O-L + Fe |
| BB-995 | 87 wt% Fe + 13 wt% S + H | 6 | Re | 960 | 4544 | Un-melted |
| BB-999 | 87 wt% Fe + 13 wt% S + H | 6 | Re | 965 | 1440 | S-L + Fe + Un-melted |
| BB-960 | 87 wt% Fe + 13 wt% S + H | 6 | Re | 980 | 102 | S-L + Fe |
| TT-793 | 87 wt% Fe + 13 wt% S + H | **8** | Re | 925 | 307 | Un-melted |
| TT-794 | 95 wt% Fe + 5 wt% S + H | **8** | Re | 950 | 369 | S-L + Fe + Un-melted |

Melting transitions in bold boxes.

the inter-lab variability and place better constraints on the eutectic temperatures in the Fe-S and Fe-S-H-O systems. We find that O and pressure are not active agents for freezing point depression, in contrast to H, which is. The potential importance of H as a freezing point depression agent for both the core (Sakamaki et al. 2009) and the base of the mantle (Nomura et al. 2014) is a recurrent theme in recent literature.

## EXPERIMENTAL AND ANALYTICAL METHODS

### Starting Materials

Troilite (FeS) was synthesized from a mix of S and Fe in equimolar proportions. This mixture was placed in a silica tube, which was then evacuated and sealed with an $H_2$-$O_2$ torch. The sealed silica tube was then placed in a furnace and heated to 950 °C at a rate of 200 °C $h^{-1}$. It was held at 950 °C for 60 min and then cooled. The combination of S with Fe reduced the vapor pressure from that of free S. The resulting solid was then ground to powder in an agate mortar under acetone. For the Fe-S experiments, reduced Fe metal was added to attain the desired mixture of Fe and FeS. For the Fe-S-O experiments, FeO was also added to attain the desired mixture of Fe, FeO, and FeS. For the Fe-S-H experiments, the Fe-S starting material was used and a layer of equimolar brucite + $MgH_2$ was added between the Fe-S and the thermocouple. The experimental methods used are similar to those discussed in Lazar et al. (2004). The starting mixtures investigated were 87 wt% Fe, 13 wt% S, and 95 wt% Fe, 5 wt% S for the Fe-S and Fe-S-H experiments. The bulk composition of the Fe-S-O experiments was 4 wt% O, 11 wt% S, and 85 wt% Fe (Table 1).

### Experimental Design and Procedure

#### *Equilibrium Experiments*

All experiments were conducted in a multianvil press. Experiments were performed in high-purity MgO capsules surrounded by high-density $LaCrO_3$ or Re heaters within precast Ceramacast 584OF octahedral pressure media with integral gaskets for 8 mm truncated edge length tungsten carbide anvil cubes. All ceramic media were dried under $N_2$ gas at 900 °C for at least 24 h to ensure that moisture was minimized in the experiments. A Type-D W/Re thermocouple was placed perpendicular to the heater axis through the heater, a couple of mm from the midpoint, to ensure that the thermocouple and the charge were at approximately symmetrical places in the heater's thermal profile. This way the experiment and the thermocouple are at the same temperature, rendering the experiment temperatures more accurate in the presence of the inevitable temperature gradients within the heaters. For the case of Re heaters and Fe-S-H experiments, the brucite + $MgH_2$ starting material between the thermocouple and the Fe-S charge was at the hot spot of the heater at a temperature above that of the thermocouple and the Fe-S charge.

Sintering at pressure was performed to close pore space in the MgO capsule, to reduce sulfide liquid leakage during equilibration. In the Fe-S experiments, sintering was undertaken at 800–900 °C for more than 4 h. Fe-S-O experiments were sintered for more than 1 h.

Fe-S-H experiments did not undergo a sintering step, but were rapidly raised from 400 °C to the run temperature. This was done to attempt to limit the loss of H before melting. A long sinter at 900 °C would liberate the $H_2$ from the starting $MgH_2 + Mg(OH)_2$ and let it escape before the pore space sintered closed or before the melting to be observed in the presence of $H_2$ could occur. Pt and Au capsule experiments were used to verify that $MgH_2 + Mg(OH)_2 \rightarrow 2MgO + 2H_2$ occurs below the run temperature of the Fe-S-H experiments. These experiments show that the reaction occurs by 600 °C (Table 1) ensuring that H is available for the eutectic experiments.

Fe-S and Fe-S-O experiments at 6 GPa used $LaCrO_3$ heaters as done by Buono and Walker (2011). In these experiments, compression to 6 GPa was accomplished through an applied force of 300 tons. All of the Fe-S-H experiments, as well as the Fe-S experiments at 8 GPa, were run using Re heaters. The Fe-S-H experiments in Re heaters at 6 GPa had 235 tons of applied force, and all of the experiments at 8 GPa with a Re heater had 300 tons of applied force.

All experiments were equilibrated for a minimum of 66 min. The charges were then quenched to 100 °C in <5 s by cutting the power to the heater. Charges were potted in epoxy and sectioned along the long axis of the heater so that the charge and the thermocouple could be studied simultaneously. The charges were polished with 0.3 μm $Al_2O_3$ powder for optical and microprobe analysis. Both the 6 and 8 GPa data are reported in Table 1.

### *Brucite + $MgH_2$ Breakdown*

We verified the breakdown of magnesium hydride ($MgH_2$) + brucite ($Mg(OH)_2$) to periclase (MgO) + $H_2$ in experiments conducted in Pt and Au capsules, which were cold welded under argon to ensure that the process of welding the capsules did not cause brucite + $MgH_2$ to break down. A metal tube 2.4 mm in diameter and wall thickness of 0.18 mm was cut; the bottom was triple-crimped and welded. The capsule was then packed with the brucite + $MgH_2$ mix used in the Fe-S-H experiments. The top of the capsule was then triple-crimped and welded closed. The capsule was then inserted within an alumina sleeve loaded into the 8 mm TEL octahedron. The setup for these experiments is the same as the one described in the Equilibrium Experiments section for $LaCrO_3$ heaters.

## Analysis of the Run Products

### *Electron Probe Microanalyzer*

An electron probe microanalyzer (EPMA; Cameca SX-100 instrument) at the American Museum of Natural History (AMNH) used a 30 μm × 30 μm or 15 μm × 15 μm raster mode beam with a 15 kV accelerating voltage at 40 nA beam current to analyze our charges. Pure Fe wire, troilite, and hematite were used as the standards. O was analyzed using the LPC2 crystal, S on the LPET, and Fe on the LLIF. In all samples, the liquid composition is uniform at 15–30 μm scale, but locally heterogeneous, consisting of quench Fe-rich dendrites surrounded by S-rich liquid mostly crystallized as troilite.

The average composition of the S-bearing liquid in each experiment was calculated and reported in Table 1. All Fe-FeS experiments displayed spatial phase separation between crystalline Fe and S-bearing liquid, allowing traverse analysis of liquid without worry of contamination from the Fe-crystal phase. This separation is the result of a slight temperature gradient (order of <10 °C $mm^{-1}$), which causes thermal migration and crystallization of Fe at the cold end. Crystal-free liquid accumulates at the warmer end. When decompression occurs after temperature quenching, the sample splits along this boundary, leaving a gap tens of microns wide. The area adjacent to this gap was avoided during microprobe analyses. Fe crystals accommodate minimal S in their structure at 6 and 8 GPa. As a result, any S left in the vicinity of the Fe phase is locally concentrated by rejection as quench growth adds S-free material to the large crystals of Fe. In all of our experiments, O and S counts in the metal phase were less than 3 times the background and thus indistinguishable from zero.

### *X-Ray Diffraction*

X-ray diffraction (XRD) measurements were completed on a Rigaku microfocusing XRD located at the AMNH. Cu Kα X-rays with a tube voltage of 46 kV and current of 40 mA were passed through a 0.8 mm collimator. Data were processed using AreaMax and Jade 7.0 software. XRD confirms that the Fe-free starting composition phases and the run product phases of the Pt and Au capsule experiments were as reported in Table 1.

# RESULTS

The experimental conditions, the resulting phase assemblages, and the run times are given in Table 1. Representative textures of the experimental charges are shown in Fig. 1 and the compositions of the resulting S-rich liquid phases (S-L) are given in Table 2.

## Phase Assemblage, Texture, and Melt Composition

### *Fe-S*

When melting occurred in the 6 GPa Fe-S system experiments at approximately 990 ± 10 °C, the phases

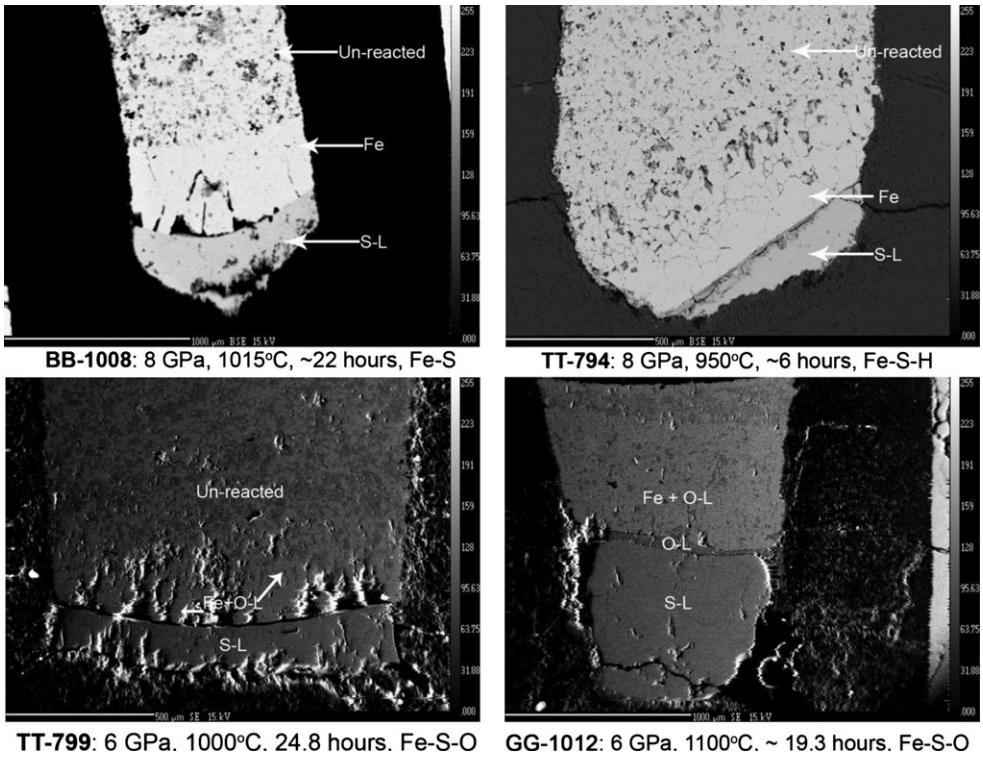


Fig. 1. BSE images for the Fe-S (top left), Fe-S-H (top right), Fe-S-O eutectic experiment (bottom left), and Fe-S-O experiment at a higher $T$ to illustrate the O-L layer formation (bottom right).

Table 2. Probe results for the S-liquid in liquid-bearing experiments (oxygen $\leq$ detection limit of 0.7%).

| Experiment # | System | $P$ (GPa) | Fe wt% | S wt% | $T$ (°C) |
|---|---|---|---|---|---|
| BB-888 | Fe-S | 6 | 77.9 | 22.1 | 1000 |
| BB-1006 | Fe-S 1st melt | 8 | NA | NA | 995 |
| BB-1008 | Fe-S | 8 | 78.6 | 21.4 | 1015 |
| GG-1012 | Fe-S-O | 6 | 77.6 | 22.4 | 1100 |
| TT-799 | Fe-S-O | 6 | 75.7 | 24.3 | 1000 |
| BB-1001 | Fe-S-H 1st melt | 6 | NA | NA | 960 |
| BB-999 | Fe-S-H | 6 | 76.0 | 24.0 | 965 |
| BB-960 | Fe-S-H | 6 | 79.4 | 20.6 | 980 |
| TT-794 | Fe-S-H | 8 | 79.6 | 20.4 | 950 |

present were Fe-S liquid and Fe metal. When melting occurred in the 8 GPa experiments, the temperature within a Re heater decreased rapidly with distance from the center of the heater. This leaves part of the charge unreacted. The portion of the charge that was at the desired run temperature had pure Fe in equilibrium with Fe-S liquid (Fig. 1). Melt compositional data are available in Table 2. The occurrence of first melt at 8 GPa (BB-1006, melting started by approximately 995 °C) had a small and dispersed liquid section, which made it difficult to get reasonable compositional data. Another experiment at a slightly higher temperature was conducted (BB-1008) to better constrain the eutectic liquid composition.

### *Fe-S-O*

All experiments in the Fe-S-O system were run at 6 GPa with $LaCrO_3$ heaters. When melting occurred, the phases present were Fe-S liquid (S-L), Fe-S-O liquid (O-L), and Fe metal. There was no measurable difference in the eutectic $T$ approximately 990 $\pm$ 10 °C between the Fe-S and Fe-S-O experiments. In TT-799, only part of the experimental charge was melted (Fig. 1). The three phase regions shown from top to bottom are unreacted bulk composition, Fe-metal, and Fe-S liquid. The Fe-S-O liquid is present as spheres within the Fe-metal section of this charge and becomes more apparent at higher $T$, when the bulk composition is more fully reacted. The O content of the S-L is below the detection limit of the EPMA. Nominal oxygen of 0.7 $\pm$ 0.3 wt% was computed from counting statistics in the S-L; however, pure Fe standard also gives 0.7 wt%, so the oxygen must be considered below reliable EMPA detection limits. Given $T$ high enough to fully react the bulk composition and long run times, the O-L (oxygen-rich liquid) will segregate into its own layer, indicating

that it is an immiscible phase, not a quench product as shown in GG-1012 (Fig. 1). Insufficient O enters the S-L at these *P–T* conditions to cause much freezing point depression. As shown in other literature regarding high-pressure studies, the effect of O on the eutectic Fe-FeS composition and *T* is minimal (Table 2) (Terasaki et al. 2011).

### *Fe-S-H*

Fe-S-H experiments at 6 GPa were initially attempted with $LaCrO_3$ heaters and abandoned because the release of H caused instability in the heater, leading to large *T* fluctuations. This feature indicates that quantitative H retention in the charge is an uncertain enterprise at best. In the Fe-S-H experiments, approximately 0.01 g of brucite + $MgH_2$ and approximately 0.015 g of Fe-FeS mixture were added to the sample capsule. Pt and Au capsule experiments at 6 GPa (Table 1) show that the conversion from brucite + $MgH_2$ to periclase + $H_2$ is completed by 600 °C. Thus, these experiments should have been flooded with $H_2$. The phases present are Fe-crystal and Fe-S liquid. Previous work (Okuchi 1997) showed that H is not retained by metallic liquids during quench, so the amount of H that entered the Fe-S is unknown and not accounted for in Table 2. It is unmeasurable with present techniques as well as being unquenchable. We can only observe its effect on freezing point depression, which is to progressively lower the eutectic temperature with pressure to below 950 °C by 8 GPa. This eutectic depression is in sharp contrast with the static, dry eutectic in Fe-S with either increased pressure or extra oxygen. In some of the Re experiments, the *T* was not high enough to react all of the Fe-S starting material, so those experiments contain Fe-S and Fe intermixed as well as the Fe metal + S-rich liquid. There is a distinct separation between the melted and unreacted segments (Fig. 1), which makes these experiments easy to probe despite some of the charge remaining unreacted.

## DISCUSSION

### Breakdown of Brucite + $MgH_2$ to 2 Periclase + 2 $H_2$

The chemical and structural simplicity of brucite has led to it being studied to outline the high-pressure behavior of hydrous minerals and the implication for the *T* and pressure of fluid release in subduction zones (Meyer and Yang 1962; Kanzaki 1991; Johnson and Walker 1993; Fukui et al. 2005; Kelkar et al. 2008). Previous work showed that the 6 GPa breakdown of brucite to periclase + $H_2O$ occurs at about 1125 °C (Johnson and Walker 1993; Fukui et al. 2005). In our Pt and Au capsule experiments with brucite + $MgH_2$, we show that the complete conversion to periclase + $H_2$ happens by 600 °C. The presence of $MgH_2$ significantly decreases the brucite stability temperature. H derived from the breakdown of $MgH_2$ lowers the dehydration *T* of brucite through dilution of the vapor with $H_2$.

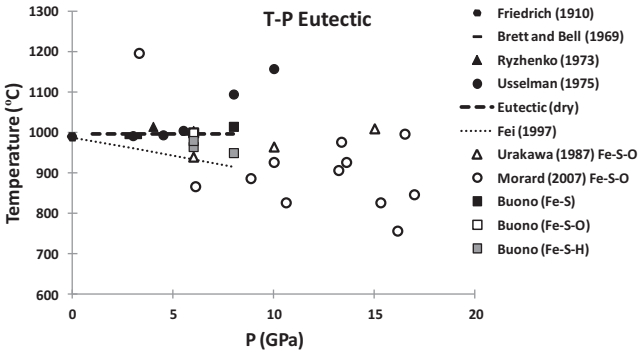


Fig. 2. Literature data for the *P* and *T* of the Fe-FeS eutectic (black filled symbols) (Friedrich 1910; Brett and Bell 1969; Ryzhenko and Kennedy 1973; Usselman 1975; Buono and Walker 2011). The dotted line is the equation given in Fei et al. (1997) for the *P* and *T* of the Fe-FeS eutectic. Also shown are the Fe-S-O system (empty symbols) (Urakawa et al. 1987; Morard et al. 2007), and the Fe-S-H system (gray squares) (this study).

### The Fe-S Eutectic

Many studies report the Fe-S eutectic (Friedrich 1910; Hansen and Anderko 1958; Brett and Bell 1969; Ryzhenko and Kennedy 1973; Usselman 1975; Fei et al. 1997; Morard et al. 2007; Buono and Walker 2011). Some of those studies report O contamination (Morard et al. 2007). Urakawa et al. (1987) looked specifically at the Fe-S-O system and described the Fe-FeS eutectic T-x up to 15 GPa (Figs. 2 and 3). These studies do not all agree on the T-P or x-P location of the Fe-FeS eutectic. This leads to uncertainty when trying to model and understand core chemistry. We believe that the presence of H, from the breakdown of $H_2O$ in the starting material and/or sample capsule/pressure media, causes some of this variability. When $H_2O$ breaks down, the O is bound to Fe making ferropericlase, which can be seen on the sample capsule wall when MgO sample capsules are used. The H is then free to interact with the Fe-FeS starting material. When Fe-S mixtures and all capsule material are rigorously dried, we find that the O content in the sample postrun is below EPMA detection limit and that there is no noticeable decrease in the eutectic temperature from 1 bar to 8 GPa. This lack of freezing point depression with pressure is also seen when dry O is added to the Fe-S system, so O is not the active ingredient causing the (erratic) decrease in Fe-S eutectic temperatures. The

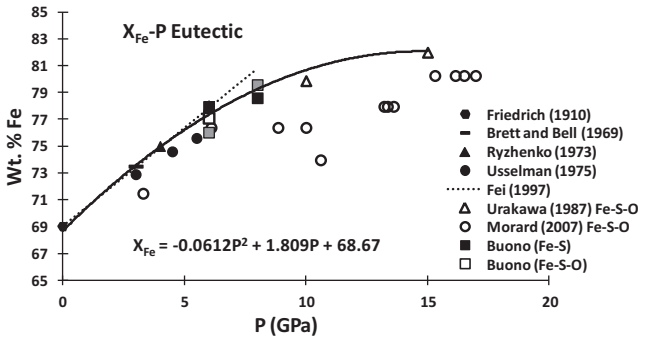


Fig. 3. Literature data for the $X_{Fe}$ and $P$ of the Fe-FeS eutectic (black filled symbols) (Friedrich 1910; Brett and Bell 1969; Ryzhenko and Kennedy 1973; Usselman 1975; Buono and Walker 2011). The dotted line is the equation given in Fei et al. (1997) for the $P$ and $T$ of the Fe-FeS eutectic. Also shown are the Fe-S-O system (empty symbols) (Urakawa et al. 1987; Morard et al. 2007), and the Fe-S-H system (gray squares) (this study). The polynomial fit to the data excludes Morard et al. (2007) and the 6–8 GPa experiments of Usselman (1975) as they are significantly different from all other literature values.

observation of ferropericlase rims on the inside of MgO capsules that are only nominally dried, for instance just by storage in a vacuum oven at 120 °C, is long-standing and somewhat mysterious because the oxygen needed to put Fe from the metallic charge into ferropericlase solution is difficult to identify. Indeed, Fig. 2A in O'Neill et al. (1998) shows a substantial ferropericlase rim for which the oxygen required is difficult to account. Majewski and Walker (1998) show a narrow ferropericlase rim in the lower right of Fig. 3A on a 3 min duration run, too rapid for diffusion into MgO to be operative even given an oxygen source. Dasgupta et al. (2013) show in Fig. 2A a ferropericlase rim on their charge, which may be partially accounted for by the initial presence of partially oxidized silicate. These examples show that ferropericlase rims are widely present in the literature, but often ignored. It is possible that the occluded moisture mechanism may provide part of the oxygen source needed for their formation. It is also possible that some Fe powder starting materials may carry a small amount of contaminant surface oxidation. However, an important observation in the present work is that these rims do not develop in rigorously dried charges unless oxygen is specifically added as in the Fe-S-O experiments.

### *Pressure (?) Effect on Eutectic Temperature*

In the Fe-S system at 6 and 8 GPa, the eutectic $T$ is 990 ± 10 °C. This is the same as it is at 1 bar and is in agreement with some of the literature data (Friedrich 1910; Hansen and Anderko 1958; Brett and Bell 1969; Ryzhenko and Kennedy 1973; Usselman 1975) (Fig. 2). Our modest excursions to 6 GPa into dry Fe-S-O do not change this result: the eutectic remains at 990 ± 10 °C. In the Fe-S-H system, however, there is a noticeable decrease in the eutectic temperature. This decrease occurs without detectable O in the S-L. The eutectic $T$ decreases as pressure increases when H is present. The decreases observed are similar to, but slightly smaller than, earlier results for the Fe-FeS system (Fei et al. 1997). The addition of H may help explain the depressed scatter in some of the literature eutectic values (Morard et al. 2007), but not the increase in eutectic $T$ at 8 GPa seen by others (Usselman 1975). The internally well-behaved results of Fei et al. (1997) call for a reproducible level of moisture for the consistent decrease in eutectic $T$ with increasing P. While none of these literature studies specifically added either H or O, it is our contention that moisture contamination will produce the H result (as O alone will not) because the O from $H_2O$ combines with Fe to make FeO (in ferropericlase) or immiscible oxide liquid.

### *Pressure Effect on Eutectic Composition*

All data sets show a continuous decrease in the wt% Fe of the liquid as pressure increases at a given $T$ (Fig. 3). For all data sets other than Morard et al. (2007) and the 8 and 10 GPa experiments of Usselman (1975), the eutectic composition can be fit quite well by a second-order polynomial (Fig. 3).

$$\text{Weight \% Fe} = -0.0612 * P^2 + 1.809 * P + 68.67 \quad R^2 = 0.956 \tag{1}$$

In this equation, pressure ($P$) is in GPa. This relationship applies up to 15 GPa. Equation 1, in combination with the eutectic $T$ of 990 °C up to at least 8 GPa, supplies reasonable constraints on Fe-FeS eutectic $T$ and x for future core formation models. This equation in combination with the model supplied in previous work (Buono and Walker 2011) will allow accurate models of the Fe-rich side of the Fe-FeS phase diagram to at least 8 GPa including the eutectic $T$, which was not previously addressed.

## 6 GPA FE-S-H SYSTEM

When our 6 GPa eutectic is plotted with the 6 GPa Fe-S-H system literature data (Fukai et al. 2003; Shibazaki et al. 2010), we can construct a simplistic, H-excess phase diagram plotted on the Fe-FeS binary. This can be compared to the H-free system at 6 GPa (Buono and Walker 2011) (Fig. 4). In the presence of

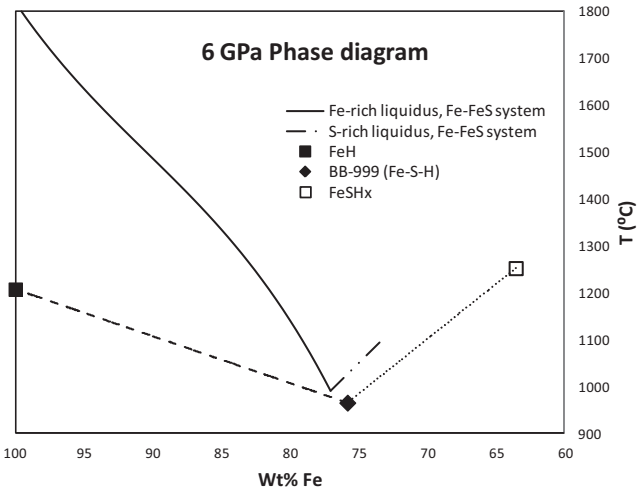


Fig. 4. The 6 GPa phase diagram for the Fe-FeS system (Buono and Walker 2011) and the FeH-$FeSH_X$ system with excess H, projected from H (Fukai et al. [2003] and Shibazaki et al. [2010] for the crystalline endmembers; and this study for the eutectic).

H, also derived from brucite + $MgH_2$ as we have done, Fukai et al. (2003) found that the melting $T$ of Fe at 6 GPa decreases by approximately 500 °C. H decreases the 6 GPa melting $T$ of FeS by approximately 100 °C (Shibazaki et al. 2010). By contrast, we show here that the 6 GPa eutectic $T$ decreases by only approximately 30°. Therefore, the melting interval shrinks in the presence of $H_2$. If the core of a smaller planetary body were composed of Fe-S-H rather than Fe-S, the temperature interval in which a solid inner core and liquid outer core could coexist would be much smaller, and would extend to only slightly lower temperatures than in Fe-S. The Fe-S-H system may apply to small icy planetary bodies with intrinsic magnetic fields.

## CONCLUSIONS

Some of the inter-lab variability for eutectic measurements with pressure may be caused indirectly by $H_2O$ contamination. $H_2O$ decomposes into $H_2$ + O. O bonds with Fe to make ferropericlase. If excess O is present, a second immiscible liquid may form (Tsuno et al. 2007). H liberated from $H_2O$ enters the melt, causing the melting point depression that is seen in some experimental results. Our dry experiments indicate that the eutectic $T$ in the Fe-S system remains undepressed at 990 ± 10 °C to at least 8 GPa. As a result, we present better constraints on the conditions for planetary core formation in small planets and moons such as Ganymede. This study increases slightly the high-pressure Fe-S eutectic $T$ commonly used and provides the possibility to drastically decrease the melting interval by moving into the ternary Fe-S-H system.

*Acknowledgments*—Mike Drake is remembered as a friend and sustainer of scientific cooperation. We would like to thank Mike Drake for also demonstrating that attention to experimental detail need not be sacrificed to conformity (Drake and Holloway 1982). We also thank him for reminding us that the objective should always be toward illuminating a bigger picture, an objective he often achieved, even as he devoted much effort and energy to the panel and committee work that shaped the local and national research environment. We acknowledge with thanks the debt owed to him by ourselves as part of a wider community. We thank two anonymous reviewers and editors John Jones and Kevin Righter for their comments. This work was supported by the U.S. National Science Foundation and is LDEO contribution 7836.

*Editorial Handling*—Dr. Kevin Righter

## REFERENCES

Anderson O. L. and Isaak D. G. 2002. Another look at the core density deficit of Earth's outer core. *Physics of the Earth and Planetary Interiors* 131:19–27.

Anderson J. D., Lau E. L., Sjogren W. L., Schubert G., and Moore W. B. 1996. Gravitational constraints on the internal structure of Ganymede. *Nature* 384:541–543.

Anderson J. D., Lau E. L., Sjogren W. L., Schubert G., and Moore W. B. 1997. Europa's differentiated internal structure: Inferences from two Galileo encounters. *Science* 276:1236–1239.

Anderson J. D., Jacobson R. A., Lau E. L., Moore W. B., and Schubert G. 2001. Io's gravity field and interior structure. *Journal of Geophysical Research* 106:32,963–32,969.

Birch F. 1952. Elasticity and constitution of the Earth's interior. *Journal of Geophysical Research* 57:227–286.

Birch F. 1964. Density and composition of mantle and core. *Journal of Geophysical Research* 69:4377–4388.

Brett R. and Bell P. M. 1969. Melting relations in the Fe-rich portion of the system Fe-FeS at 30 kb pressure. *Earth and Planetary Science Letters* 6:479–482.

Buono A. S. and Walker D. 2011. The Fe-rich liquidus in the Fe-FeS system from 1 bar to 10 GPa. *Geochimica et Cosmochimica Acta* 75:2072–2087.

Dasgupta R., Chi H., Shimizu N., Buono A. S., and Walker D. 2013. Carbon solution and partitioning between metallic and silicate melts in a shallow magma ocean: Implications for the origin and distribution of terrestrial carbon. *Geochimica et Cosmochimica Acta* 102:191–212.

Drake M. J. and Holloway J. R. 1982. Partitioning of Ni between olivine and silicate melt: The "Henry's Law" problem reexamined: Reply to a discussion by B. Mysen. *Geochimica et Cosmochimica Acta* 46:299.

Fei Y., Bertka C. M., and Finger L. W. 1997. High-pressure iron-sulfur compound, $Fe_3S_2$, and melting relations in the Fe-FeS system. *Science* 275:1621–1623.

Friedrich K. 1910. Notiz uber das Schmelzdiagramm des Systemes Schwereleisen—Eisen. *Metallurgie* 9:33–48.

Fukai Y., Mori K., and Shinomiya H. 2003. The phase diagram and superabundant vacancy formation in Fe-H alloys under high hydrogen pressures. *Journal of Alloys and Compounds* 348:105–109.

Fukui H., Inoue T., Yasui T., Katsura T., Funakoshi K. I., and Ohtaka O. 2005. Decomposition of brucite up to 20 GPa: Evidence for high MgO-solubility in the liquid phase. *European Journal of Mineralogy* 17:261–267.

Hansen M. and Anderko K. 1958. *Constitution of the binary alloys*. New York: McGraw-Hill. 1305 p.

Hillgren V. J., Gessmann C. K., and Li J. 2000. *An experimental perspective on the light element in Earth's core*. *Origin of the Earth and Moon*. Tucson, Arizona: University of Arizona Press. pp. 245–263.

Johnson M. C. and Walker D. 1993. Brucite [$Mg(OH)_2$] dehydration and the molar volume of $H_20$ to 15 GPa. *American Mineralogist* 78:271–284.

Kanzaki M. 1991. Dehydration of brucite ($Mg(OH)_2$) at high pressures detected by differential thermal analysis. *Geophysical Research Letters* 18:2189–2192.

Kelkar T., Kanhere D. G., and Pal S. 2008. First principles calculations of thermal equations of state and thermodynamical properties of $MgH_2$ at finite temperatures. *Computational Materials Science* 42:510–516.

Lazar C., Walker D., and Walker R. J. 2004. Experimental partitioning of Tc, Mo, Ru, and Re between solid and liquid during crystallization in Fe-Ni-S. *Geochimica et Cosmochimica Acta* 68:643–651.

Li J. and Fei Y. 2003. Experimental constraints on core composition. *Treatise on Geochemistry* 2:521–546.

Majewski E. and Walker D. 1998. S diffusivity in Fe-Ni-S-P melts. *Earth and Planetary Science Letters* 160:823–830.

McDonough W. F. 2003. Compositional model for the Earth's core. In *The mantle and core*, edited by Holland H. D. and Turekian K. K. Treatise on Geochemistry, vol. 2. Oxford: Pergamon. pp. 547–568.

Meyer J. W. and Yang J. C. S. 1962. Some observations in the system MgO-$H_2O$. *American Journal of Science* 260:707–717.

Morard G., Sanloup C., Fiquet G., Mezouar M., Rey N., Poloni R., and Beck P. 2007. Structure of eutectic Fe–FeS melts to pressures up to 17 GPa: Implications for planetary cores. *Earth and Planetary Science Letters* 263:128–139.

Morgan J. W. and Anders E. 1980. Chemical composition of Earth, Venus, and Mercury. *Proceedings of the National Academy of Sciences of the United States of America* 77:6973–6977.

Nomura R., Hirose K., Uesugi K., Ohishi Y., Tsuchiyama A., Miyake A., and Ueno Y. 2014. Low core-mantle boundary temperature inferred from the solidus of pyrolite. *Science* 343:522–525.

Okuchi T. 1997. Hydrogen partitioning into molten iron at high pressure: Implications for Earth's core. *Science* 278:1781–1784.

O'Neill H. St C., Canil D., and Rubie D. C. 1998. Oxide-metal equilibria to 2500 °C and 25 GPa: Implications for core formation and the light component in Earth's core. *Journal of Geophysical Research* 103(B6):12,239–12,260.

Poirier J.-P. 1994. Light elements in the Earth's outer core: A critical review. *Physics of The Earth and Planetary Interiors* 85:319–337.

Ryzhenko B. and Kennedy G. C. 1973. The effect of pressure on the eutectic in the system Fe-FeS. *American Journal of Science* 273:803–810.

Sakamaki K., Takahashi E., Nakajima Y., Nishihara Y., Funakoshi K., Suzuki T., and Fukai Y. 2009. Melting phase relation of FeHx up to 20 GPa: Implication for the temperature of the Earth's core. *Physics of the Earth and Planetary Interiors* 174:192–201.

Sanloup C., Jambon A., and Gillet P. 1999. A simple chondritic model of Mars. *Physics of The Earth and Planetary Interiors* 112:43–54.

Shibazaki Y., Ohtani E., Terasaki H., Tateyama R., Sakamaki T., Tsuchiya T., and Funakoshi K. 2010. Effect of hydrogen on the melting temperature of FeS at high pressure: Implications for the core of Ganymede. *Earth and Planetary Science Letters* 301:153–158.

Stevenson D. J. 1987. Limits on lateral density and velocity variations in the Earth's outer core. *Geophysical Journal of the Royal Astronomical Society* 88:311–319.

Stevenson D. J. 2001. Mars' core and magnetism. *Nature* 412:214–219.

Stevenson D. J. 2010. Planetary magnetic fields: Achievements and prospects. *Space Science Reviews* 152:651–664.

Terasaki H., Kamada S., Sakai T., Ohtani E., Hirao N., and Ohishi Y. 2011. Liquidus and solidus temperatures of a Fe-O-S alloy up to the pressures of the outer core: Implication for the thermal structure of the Earth's core. *Earth and Planetary Science Letters* 304:559–564.

Tsuno K., Ohtani E., and Terasaki H. 2007. Immiscible two-liquid regions in the Fe–O–S system at high pressure: Implications for planetary cores. *Physics of The Earth and Planetary Interiors* 160:75–85.

Urakawa S., Kato M., and Kumazawa M. 1987. *Experimental study on the phase relations in the system Fe–Ni–O–S*. *High-pressure research in mineral physics*. Tokyo: TERRAPUB. pp. 95–111.

Usselman T. 1975. Experimental approach to the state of the core: Part I. The liquidus relations of the Fe-rich portion of the Fe-Ni-S system from 30 to 100 kb. *American Journal of Science* 275:278–290.